



1 Improved Response Surface Method for Time-Variant Reliability 2 Analysis of Nonlinear Random Structures Under Non-Stationary 3 Excitations

4 SAYAN GUPTA and C.S. MANOHAR*

5 *Department of Civil Engineering, Indian Institute of Science, Bangalore 560012 India;*

6 **Author for correspondence (e-mail: manohar@civil.iisc.ernet.in; fax: +91-80-2360-0404)*

7 (Received: 21 July 2003; accepted: 19 January 2004)

8 **Abstract.** The problem of time-variant reliability analysis of randomly driven linear/nonlinear vibrating structures is studied. The
 9 excitations are considered to be non-stationary Gaussian processes. The structure properties are modeled as non-Gaussian random
 10 variables. The structural responses are therefore non-Gaussian processes, the distributions of which are not generally available in
 11 an explicit form. The limit state is formulated in terms of the extreme value distribution of the response random process. Developing
 12 these extreme value distributions analytically is not easy, which makes failure probability estimations difficult. An alternative
 13 procedure, based on a newly developed improved response surface method, is used for computing exceedance probabilities. This
 14 involves fitting a global response surface which approximates the limit surface in regions which make significant contributions to
 15 the failure probability. Subsequent Monte Carlo simulations on the fitted response surface yield estimates of failure probabilities.
 16 The method is integrated with professional finite element software which permits reliability analysis of large structures with
 17 complexities that include material and geometric nonlinear behavior. Three numerical examples are presented to demonstrate the
 18 method.

19 **Key words:** improved response surface method, material and geometric nonlinearity, non-Gaussian structural randomness,
 20 time-variant reliability

21 1. Introduction

22 A randomly driven vibrating structure is deemed to be safe if its responses stay below specified thresh-
 23 olds over a given duration of time, The extreme values of response processes, over a given period of time,
 24 thus play a decisive role in the evaluation of structural reliability. The theory of asymptotic distribu-
 25 tions of sequences of independent and identically distributed (i.i.d.) random variables is well developed
 26 [1–3]. This theory can be used to study the maximum values of random processes over a given period
 27 of time, by considering the random variable sequence as consisting of the local maxima of random
 28 variables. Alternatively, one can relate the extreme value of random processes over a given period,
 29 to the probability distribution of first passage times. For the case of stationary, Gaussian random pro-
 30 cesses, these two approaches lead to Gumbel models for the extreme responses [4]. In applying these
 31 formulations, one needs to know the joint probability density function (PDF) of the process and its
 32 derivative at a given instant. While the determination of this joint PDF for Gaussian random responses
 33 is straightforward, complexities would arise if the response is non-Gaussian. This might happen if
 34 the inputs are non-Gaussian, the structure is either nonlinear and/or randomly parametered. Similar
 35 problems are encountered even for linear deterministic systems under Gaussian inputs, if attention is
 36 focused on nonlinear functions of displacement response, as in the case of principal stresses or Von
 37 Mises stresses. When response processes possess Markovian properties, one can use methods based on
 38 the backward Kolmogorov equation governing the transition PDF, or the generalized Pontriagin–Vitt

2 *S. Gupta and C. S. Manohar*

(GPV) equations governing the moments of the first passage times [5]. These methods are generally applicable to structures with limited degrees of freedom.

Few studies on the exceedance probabilities of non-Gaussian random processes have been reported in the literature. A commonly studied non-Gaussian process, the exceedance probabilities of which are often required for estimating structure reliabilities, is the Von Mises stress. Obtained as a nonlinear function of the stress components, which are themselves random processes, Von Mises stress can therefore be viewed as a problem in nonlinear load combinations. Analytical expressions for the mean outcrossing rate of Von Mises stress in linear structures under Gaussian excitations have been developed [6] by invoking outcrossing approximations. Methods have also been studied [7–9] for computing the root-mean-square of Von Mises stress resulting from zero-mean, stationary Gaussian loadings, and for estimating their instantaneous exceedance probabilities. Linearizing techniques have been applied to obtain bounds on the exceedance probabilities of non-Gaussian random processes [10–12]. However, in large structures, where the finite element method is an indispensable tool for handling complexities such as geometric and/or material nonlinearities, structural randomness and non-stationary excitations – it is difficult to apply these methods as the performance function is defined in implicit form. For this class of problems, response surface-based methods provide an alternative computational procedure for estimating the exceedance probability of the response.

Response surface-based methods aim to develop approximate functions that are surrogates for long running computer codes [13, 14]. Techniques for constructing response surfaces in reliability problems can be classified in two broad categories. In methods developed from statistical sampling theory, factorial designs and regression analyses are used to fit response surfaces. This approach has been used for studying soil structure interaction problems [15, 16], static nonlinear structures [17, 18] and to obtain statistics of response for nonlinear oscillators [19]. As the design of experiments is centered around the mean and is independent of the limit surface geometry, the fitted response surface may not always conform to the true failure surface, especially when it is at a great distance from the mean. Alternative methods, which, however, bypass some of the mathematical requirements of response surfaces, obtain satisfactory results by incorporating reliability concepts for fitting the response surface in the vicinity of the design point. These methods have been widely reported in the literature for assessing the reliability of a variety of linear/nonlinear, static/dynamic problems [20–27]. It has been shown, however [28], that the failure probability estimates are highly sensitive to the algorithm parameters. Moreover, it is implicitly assumed that the contribution to the failure probability arises only from a single design point. This leads to erroneous estimates when there are multiple design points or multiple regions that make significant contributions to failure probability [29].

Recently, the present authors have been investigating the development of computational tools for time-variant reliability analysis of structures subjected to earthquake loads. These investigations include:

- 1.) Development of multivariate extreme value distributions of vector Gaussian random processes and their application to the problem of time-variant system reliability analysis [30]. This development is based on the application of the theory of multivariate point processes.
- 2.) Development of an improved response surface method that aspires to obtain a global response surface model that takes into account the possible existence of multiple design points and limit surface geometries characterized by multiple regions of comparable importance [31]. Here, an algorithm has been developed which traces the limit surface lying between two hyperspheres of specified radii in the standard normal space.

In the present study we extend the scope of the improved response surface method mentioned above, by considering the reliability analysis of nonlinear, randomly parametered dynamical systems, subjected

85 to non-stationary Gaussian excitations. The structure to be analyzed is modeled using professional finite
 86 element (FE) software, such as NISA, and external software that carries out response surface modeling
 87 and is interfaced with the FE model. The treatment of the problem includes one or more of the following
 88 complicating features:

- 89 1.) Randomness in structural parameters. Here, it is of interest to note that physical parameters—such
 90 as Young's modulus, density and strength characteristics – are strictly positive and require non-
 91 Gaussian models.
 - 92 2.) Possibility of geometric and/or material nonlinear structural behavior.
 - 93 3.) Large-scale structural models.
 - 94 4.) Response variables that are nonlinear functions of displacement response, such as the Von Mises
 95 stress.
 - 96 5.) Non-stationary random excitations.
- 97 The procedures developed are illustrated through a set of three numerical examples and are validated
 98 with the help of limited Monte Carlo simulations.

99 2. Problem Statement

100 A structure under random dynamic loads is considered. The governing equations of motion, when
 101 discretized using finite elements and expressed in a general form, are given by

$$\mathbf{M}\ddot{\mathbf{Y}}(t) + \mathbf{C}\dot{\mathbf{Y}}(t) + \mathbf{K}[\mathbf{Y}(t), \dot{\mathbf{Y}}(t)]\mathbf{Y}(t) = \mathbf{F}(t). \quad (1)$$

102 Here, $\mathbf{Y}(t)$, $\dot{\mathbf{Y}}(t)$ and $\ddot{\mathbf{Y}}(t)$ are, respectively, the n -dimensional vectors of nodal displacements, velocities
 103 and accelerations and, \mathbf{M} , \mathbf{C} and \mathbf{K} are, respectively, the global mass, damping and stiffness matrices
 104 of size $n \times n$. If geometric and/or material nonlinear behavior of the structure is considered, \mathbf{K} is a
 105 nonlinear function of $\mathbf{Y}(t)$ and $\dot{\mathbf{Y}}(t)$. $\mathbf{F}(t)$ represents the nodal force vector. For support motion problems,
 106 $\mathbf{F}(t) = -\mathbf{M}\mathbf{1}\ddot{U}_g(t)$, where $\ddot{U}_g(t)$ is the random process denoting support acceleration and $\mathbf{1}$ is the
 107 vector of participation factors, consisting of either 0 or 1. $\mathbf{F}(t)$ represents a vector of random processes
 108 characterized by the power spectral density (PSD) matrix $\mathbf{S}_{\mathbf{FF}}(\omega)$. Since the field equations constitute
 109 a system of nonlinear differential equations, time histories of the structure response are obtained from
 110 numerical time integration of Equation (1). This requires that the forcing function be expressed in the
 111 time domain. Thus, for stationary Gaussian random processes, $F_i(t)$ is expressed as a linear sum of
 112 harmonic functions with random coefficients and is of the form

$$F_i(t) = \sum_{k=1}^N \{a_{i_k} \cos(\omega_k t) + b_{i_k} \sin(\omega_k t)\}. \quad (2)$$

113 Here, $F_i(t)$ is the i th element of $\mathbf{F}(t)$, N denotes the number of terms used for discretizing $S_{F_i F_i}(\omega)$, and
 114 ω_k are the discretized frequencies. a_{i_k} and b_{i_k} are Gaussian random variables, such that $\langle a_{i_k} \rangle = \langle b_{i_k} \rangle =$
 115 $\langle F_i(t) \rangle$ and $\langle a_{i_k}^2 \rangle = \langle b_{i_k}^2 \rangle = \sigma_{i_k}^2$, where $\sigma_{i_k}^2$ is the area of the k th segment of the discretized PSD $S_{F_i F_i}(\omega)$.
 116 For correlated random processes $F_i(t)$ and $F_j(t)$, the correlation is specified through the cross-PSD
 117 function $S_{F_i F_j}(\omega)$, which, in turn, is expressed through the covariance of the random variables a_k and
 118 b_k . Non-stationary Gaussian random processes can be obtained by multiplying Equation (2) with a
 119 deterministic envelope function $e(t)$, of the form

$$e(t) = A_1[\exp(-A_2 t) - \exp(-A_3 t)]. \quad (3)$$

4 *S. Gupta and C. S. Manohar*

Here, the parameters A_2 and A_3 determine the shape of $e(t)$ and A_1 is a normalization factor such that $\max[e(t)] = 1.0$. 120 121

Let $V(t)$ be the response quantity of interest, which, in its most general form, is written as 122

$$V(t) = h[\mathbf{Y}(t), \dot{\mathbf{Y}}(t), \ddot{\mathbf{Y}}(t)]. \quad (4)$$

Thus, even in linear structures under Gaussian excitations, if $h[\cdot]$ is a nonlinear function, determining 123 the probability distribution of $V(t)$ is not easy, even though the probability distributions of $\mathbf{Y}(t)$, $\dot{\mathbf{Y}}(t)$ 124 and $\ddot{\mathbf{Y}}(t)$ are known exactly. Examples of such processes are the principal stress components and Von 125 Mises stress. For structures which behave nonlinearly, or when \mathbf{M} , \mathbf{C} , \mathbf{K} are randomly parametered, 126 the task is even more difficult as the distributions of $\mathbf{Y}(t)$, $\dot{\mathbf{Y}}(t)$ and $\ddot{\mathbf{Y}}(t)$ are themselves not available 127 explicitly. Failure probability is formulated as the complement of probability of $V(t)$ exceeding a 128 specified threshold α in the interval $[0, T]$, where T is the duration of interest. Mathematically, this is 129 expressed as 130

$$P_f = 1 - P[V(t) \leq \alpha; \forall t \in (0, T)]. \quad (5)$$

Here, α could also be random. Introducing the random variable $V_m = \max_{0 \leq t \leq T} V(t)$, the time-dependent 131 reliability problem can be rewritten in the time-independent format as 132

$$P_f = 1 - \int_{-\infty}^{\infty} \left\{ \int_{-\infty}^{\alpha} p_{v_m}(v) dv \right\} p_{\alpha}(a) da, \quad (6)$$

where, $p_{\alpha}(\cdot)$ is the pdf of α . If the joint PDF of $V(t)$ and $\dot{V}(t)$ is known, $p_{v_m}(v)$ can be deter- 133 mined from the outcrossing approach, and estimates of P_f can be obtained from Equation (6). 134 However, in most situations, the distribution of $V(t)$ is not available. The problem is then for- 135 mulated in the space spanned by the vector of basic random variables $\mathbf{Z} = [\mathbf{Z}_L, \mathbf{Z}_S, \alpha]$, which 136 maybe correlated and non-Gaussian. Here, \mathbf{Z}_L and \mathbf{Z}_S are, respectively, the vectors of random vari- 137 ables denoting randomness in load and structure properties. The failure probability is expressed 138 as 139

$$P_f = \int_{\tilde{g}(\mathbf{Z}) < 0} p_{\mathbf{z}}(\mathbf{z}) d\mathbf{z}. \quad (7)$$

Here, the limit surface is represented as $\tilde{g}(\mathbf{Z}) = \alpha - V_m(\mathbf{Z}_L, \mathbf{Z}_S) = 0$. Obtaining analytical expres- 140 sions for P_f becomes difficult, especially when $\tilde{g}(\mathbf{Z})$ is a highly nonlinear function and is implicitly 141 defined. In this study, exceedance probabilities of structural response are obtained from Equation (7) by 142 adopting an improved response surface method. Details of the algorithm used are outlined in the next 143 section. 144

3. Improved Response Surface Method 145

The basic idea here is to trace the limit surface lying between two hyperspheres of specified radii in 146 the standard normal space. The details of this formulation have been discussed in a recent paper by the 147 present authors [31]. Here we provide a brief description of the key ideas. Figure 1 provides a schematic 148 illustration of these steps: (1) Define the performance function, $g(\mathbf{X})$, in the M -dimensional standard 149 normal space \mathbf{X} , by transforming the problem from the M -dimensional \mathbf{Z} space. (2) Use Bucher and 150

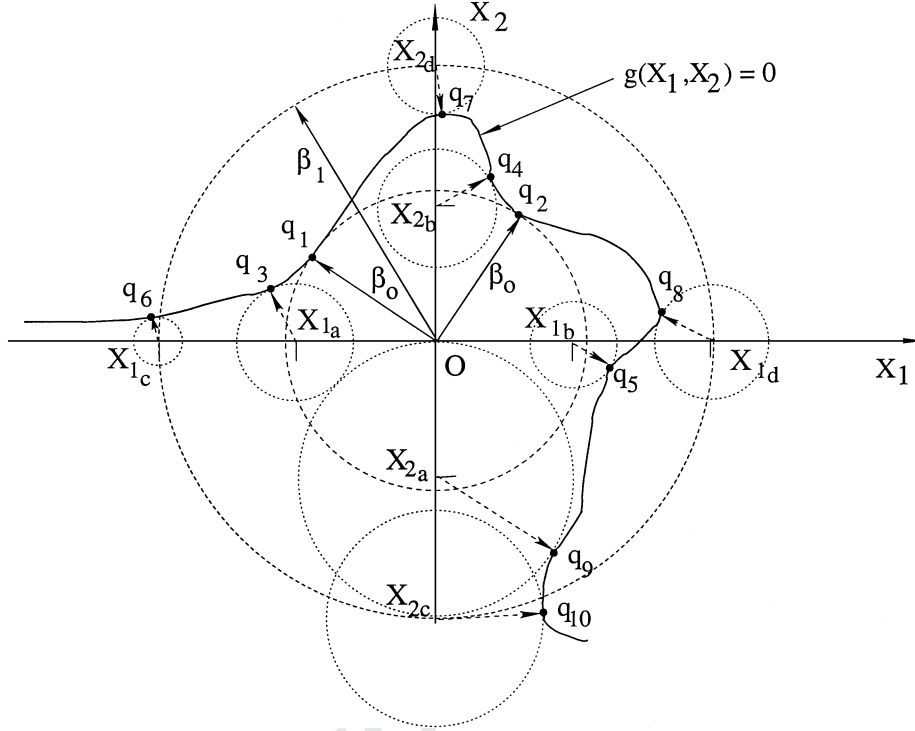


Figure 1. Schematic description of the proposed method: q_i , ($i = 1, \dots, 10$) are the points identified on the limit surface, q_1 and q_2 are multiple design points, $q_3, q_4, q_5, q_8, q_7, q_6, q_9, q_{10}$ are points arranged in decreasing order of importance in evaluating failure probability.

151 Bourgund's algorithm to identify the design point, q_1 , on $g(\mathbf{X}) = 0$. (3) Compute the Hasofer-Lind
 152 reliability index, β_0 , corresponding to q_1 . (4) Shift the origin O along the i th axis, ($i = 1, \dots, M$)
 153 to O_{ij} such that the i th coordinate of the shifted origin is given by $u_{ik} = u_{i0} + (-1)^j(j-1)d$. Here,
 154 i denotes the shift along the i th axis, j denotes the j th, ($j = 1, \dots, k$) shift along axis i and u_{i0}
 155 is the i th coordinate of O . The distance $d = (\beta_1 - (-\beta_1))/k$ where $\beta_1 = -\Phi^{-1}[10^{-4}\Phi(-\beta_0)]$ and k
 156 is the number of shifts along the i th axis. (5) Define the performance function with respect to O_{ij} .
 157 Use Bucher and Bourgund's algorithm to identify the design point q_i in the new coordinate system.
 158 Transform the coordinates of q_i to the original standard normal space. (6) Repeat steps (4) and (5)
 159 by shifting the origin k times along each of the M axes. A total of $R = kM + 1$ points are thus
 160 identified, where $g(\mathbf{X}) \approx 0$. The total number of $g(\mathbf{X})$ evaluations required is $(4M + 3)(1 + kM)$. (7)
 161 Fit an l th order polynomial through these R points. If cross terms are neglected, the polynomial is of
 162 the form

$$G = a_0 + \sum_{i=1}^M a_i X_i + \sum_{i=1}^M b_i X_i^2 + \sum_{i=1}^M c_i X_i^3 + \dots \text{ upto } l\text{th order.} \quad (8)$$

163 Here, the number of unknown coefficients is $lM + 1$, such that $lM + 1 \leq R$. The $(lM + 1) \times 1$
 164 vector of unknown coefficients, \mathbf{D} , is obtained from the equation $\mathbf{G} = \mathbf{ZD}$, where, $g(\mathbf{X})$ evaluated at
 165 the R points constitutes the $(R \times 1)$ vector \mathbf{G} and \mathbf{Z} is an $R \times (lM + 1)$ dimensional matrix, given

6 *S. Gupta and C. S. Manohar*

by

166

$$\mathbf{Z} = \begin{bmatrix} 1 & X_{1a} & X_{2a} & \dots & X_{1a}^2 & X_{2a}^2 & \dots & X_{1a}^l & X_{2a}^l & \dots \\ 1 & X_{1b} & X_{2b} & \dots & X_{1b}^2 & X_{2b}^2 & \dots & X_{1b}^l & X_{2b}^l & \dots \\ \dots & \dots & \dots & \dots & \dots & \dots & \dots & \dots & \dots & \dots \\ 1 & X_{1r} & X_{2r} & \dots & X_{1r}^2 & X_{2r}^2 & \dots & X_{1r}^l & X_{2r}^l & \dots \end{bmatrix}. \quad (9)$$

If cross terms are considered in Equation (8), the number of unknown coefficients increases and \mathbf{Z} needs to be adjusted accordingly. A least-square estimate of the unknown coefficients \mathbf{D} , is obtained from the equation

$$\hat{\mathbf{D}} = E[\mathbf{D}] = (\mathbf{Z}'\mathbf{Z})^{-1}\mathbf{Z}'\mathbf{G}. \quad (10)$$

For $(\mathbf{Z}'\mathbf{Z})$ to be invertible, all rows in \mathbf{Z} which are identical (within a given tolerance) need to be eliminated. (8) Perform Monte Carlo simulations on the response surface and estimate P_f from the relative frequency of failures.

The points identified by the algorithm lie close to the failure surface. The fitted response surface is thus expected to have a good correspondence to the geometry of the limit surface. This also takes into account the effect of multiple design points and/or regions which make significant contributions to failure. Hence, Monte Carlo simulations on the fitted response surface yield realistic estimates of P_f . The following numerical examples are presented to demonstrate the applicability of the method in time-variant reliability problems.

4. Numerical Examples

Three examples are presented to illustrate the procedures described in the previous section. The failure estimates have been compared through the following three procedures: (1) *Method 1*: An estimate of P_f is obtained from the relative frequency of failures obtained from full scale Monte Carlo simulations on the exact performance function. This involves the analysis of an ensemble of response time histories obtained by direct integration of Equation (1), for a set of sample time histories of excitation $F(t)$. The accuracy of the estimate of reliability obtained using this method depends upon the sample size used. Notwithstanding this fact, we take the results from this analysis to be the benchmark against which other approximate procedures can be evaluated. (2) *Method 2*: An estimate of P_f is obtained from the Hasofer–Lind reliability index, computed by fitting a response surface using Bucher and Bourgund's algorithm. (3) *Method 3*: Estimates of P_f are obtained by adopting the improved response surface procedure.

4.1. EXAMPLE 1: A SINGLE DEGREE OSCILLATOR WITH BILINEAR STIFFNESS

A single-degree-of-freedom oscillator, under random harmonic, non-stationary excitations, is studied. The governing equation of motion is of the form

$$m\ddot{y}(t) + c\dot{y}(t) + F_r[y(t)] = F(t), \quad (11)$$

194 where $F_r[y(t)]$ is a nonlinear conservative restoring force developed in the spring, given
195 by

$$\begin{aligned} F_r[y(t)] &= k_1 y_t + k_2 [y(t) - y_t] \quad \text{for } y(t) > y_t \\ &= k_1 y(t) \quad \text{for } -y_t \leq y(t) \leq y_t \\ &= -k_1 y_t + k_2 [y(t) + y_t] \quad \text{for } y(t) < -y_t. \end{aligned} \quad (12)$$

196 Here, y_t is a threshold displacement. The random forcing function is expressed as $F(t) = e(t)A \sin(\omega t)$,
197 where $e(t)$ is of the form in Equation (3), A denotes the random amplitude of the harmonic excitation, and
198 ω is the random excitation frequency. Consequently, A and ω are random variables. Numerical values of
199 the envelope parameters A_i ($i = 1, 2, 3$) are taken to be 10.8448, 0.35 and 0.80, respectively. The time
200 duration of excitation T is 20 s and $t_{\text{peak}} = 1.85$ s. The randomness in the system is expressed through
201 an 8-dimensional vector of random variables \mathbf{X} . These variables are listed in Table 1 together with the
202 details of the assumed type of distributions. Failure is defined to occur when $F_r[y(t)]$ exceeds a specified
203 threshold α within the interval $[0, T]$. The performance function is written, as in Equation (5), where
204 $V(t)$ represents $F_r[y(t)]$. Time histories of $F_r[y(t)]$ are obtained by solving the nonlinear differential
205 Equation (11) numerically.

206 Estimates of the exceedance probabilities computed by methods 1–3 and are illustrated in Figure 2.
207 A sample size of 2000 was considered for Monte Carlo simulations in Method 1. The parameters
208 considered in Method 3 for fitting the response surface are $k = 3$, $l = 2$ and $h = 3$ and the sample size
209 for performing Monte Carlo simulations on the fitted response surface is taken to be 2000. The number
210 of $g(\mathbf{X})$ evaluations required in Methods 1–3 are, respectively 2000, 35 and 875. It should be noted
211 that the major computational effort required in Method 3 is in fitting the response surface and hence,
212 the sample size for Monte Carlo simulations on the fitted response surface is not a restrictive factor in
213 terms of CPU usage.

214 4.2. EXAMPLE 2: LINEAR STRUCTURE WITH RANDOM PARAMETERS

215 A 1.5 m long cantilever beam, under non-stationary random support motion, is studied. The beam cross-
216 sectional dimensions are 0.15×0.03 m. The finite element method is used for structural analysis. The
217 beam is discretized using ten of 4-noded plane stress elements, with each node having two translational
218 degrees of freedom. The structure matrices are of dimensions 40×40 . The first four structure natural

Table 1. Distributional properties of the random variables in example 1.

Random variable	Probability distribution	Mean	Coefficient of variation
m	lognormal	1×10^6 kg	0.03
c	lognormal	4.38×10^5 kg-s	0.30
k_1	lognormal	30×10^6 N/mm	0.03
k_2	lognormal	54×10^6 N/mm	0.05
y_t	lognormal	0.010 mm	0.05
A	Gaussian	1×10^4 mm	0.30
ω	lognormal	5 rad/s	0.03
α	lognormal	$2.0 \times 10^5 - 2.8 \times 10^5$ N	0.03

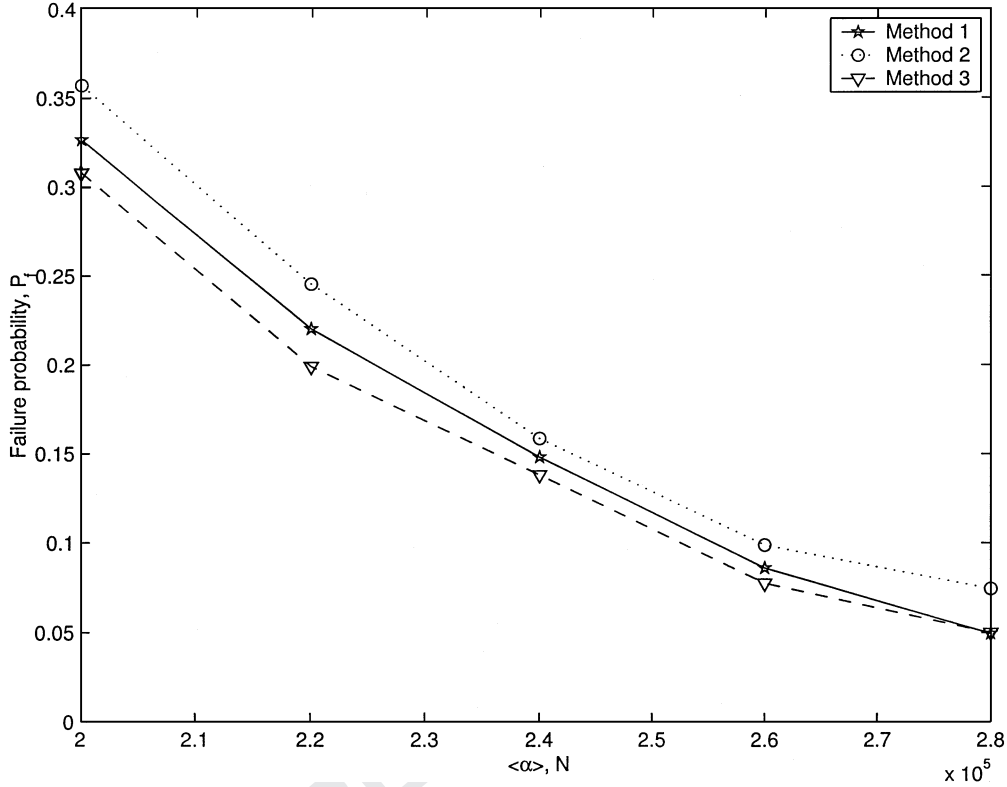
8 *S. Gupta and C. S. Manohar*

Figure 2. Exceedance probability estimates for a nonlinear oscillator under non-stationary excitations; example 1.

frequencies are 450, 1202, 1839 and 2278 rad/s, respectively. The PSD of support acceleration, $\ddot{U}_g(t)$, 219
is taken to be of the form 220

$$S_{\ddot{U}_g \ddot{U}_g}(\omega) = S_0 \frac{1 + 4\eta_g^2(\omega/\omega_g)^2}{[1 - (\omega/\omega_g)^2]^2 + 4\eta_g^2(\omega/\omega_g)^2} \quad (13)$$

where $\omega_g = 1500$ rad/s, $\eta_g = 1.2$ and ω is the frequency of excitation. It is observed that 221
 $\max[S_{\ddot{U}_g \ddot{U}_g}(\omega)]$ occurs at $\omega = 1447$ rad/s. Non-stationary time histories for support acceleration are 222
generated from Equations (2) and (3), with $N = 5$. The frequencies at which $S_{\ddot{U}_g \ddot{U}_g}(\omega)$ has been 223
discretized are 450, 1202, 1447, 1839 and 2200 rad/s. The parameters $A_i (i = 1, 2, 3)$ in Equation 224
(3) are taken to be 7.1820, 60 and 41, respectively. The peak support acceleration is observed at 225
 $t_{\text{peak}} = 0.02$ s. 226

Failure is defined to occur on initiation of yielding, when the Von Mises stress exceeds the 227
material yield stress, which, for all practical purposes, denotes the limit of linear material be- 228
havior in ductile materials. The performance function is defined in terms of the Von Mises 229
stress developed at the root of the cantilever beam and is of the form given in Equation (5). 230
Here, $V(t)$ is the Von Mises stress, given by $V(t) = (\sigma(t)\mathbf{A}\sigma(t))^{0.5}$, α is the yield stress, 231
the time duration $T = 0.04$ s, $\sigma(t) = [\sigma_{xx}\sigma_{yy}\sigma_{zz}\sigma_{xy}\sigma_{yz}\sigma_{xz}]^T$ is the nodal stress vector 232

233 and

$$\mathbf{A} = \begin{bmatrix} 1 & -0.5 & -0.5 & 0 & 0 & 0 \\ -0.5 & 1 & -0.5 & 0 & 0 & 0 \\ -0.5 & -0.5 & 1 & 0 & 0 & 0 \\ 0 & 0 & 0 & 3 & 0 & 0 \\ 0 & 0 & 0 & 0 & 3 & 0 \\ 0 & 0 & 0 & 0 & 0 & 3 \end{bmatrix}. \quad (14)$$

234 The structure material is assumed to have mass density 7850 kg/m^3 , Poisson's ratio 0.30 and proportional
 235 damping, assumed to be 5% in the first two modes, is considered. The randomness in Young's modulus
 236 (E) and yield stress (α) are expressed as $E = E_0(1 + \epsilon_1 Z_1)$ and $\alpha = \alpha_0(1 + \epsilon_2 Z_2)$, where, E_0 and
 237 α_0 respectively, denote the deterministic components of E and α . ϵ_1 and ϵ_2 are small deterministic
 238 constants, taken to be equal to 0.05 . Z_1 and Z_2 are assumed to be lognormal random variables, such
 239 that $\langle Z_1 \rangle \geq 2.0$, $\langle Z_2 \rangle \geq 0.1$, $\sigma_{Z_1} = 1.0$ and $\sigma_{Z_2} = 0.05$, where σ_{z_i} denotes the standard deviation of
 240 random variables z_i ($i = 1, 2$). The performance function is thus defined in a 12-dimensional random
 241 variable space. The constant S_0 in Equation (13) is varied from 40 to $80 \text{ m}^2/\text{s}^3$ and the corresponding
 242 failure probability estimates, computed by Methods 1–3, are shown in Figure 3. A sample size of 3000
 243 has been considered for Monte Carlo simulations in Method 1. The numerical values of the parameters
 244 used in Method 3 are $k = 6$, $l = 2$, $h = 1$ and the sample size for Monte Carlo simulations on the

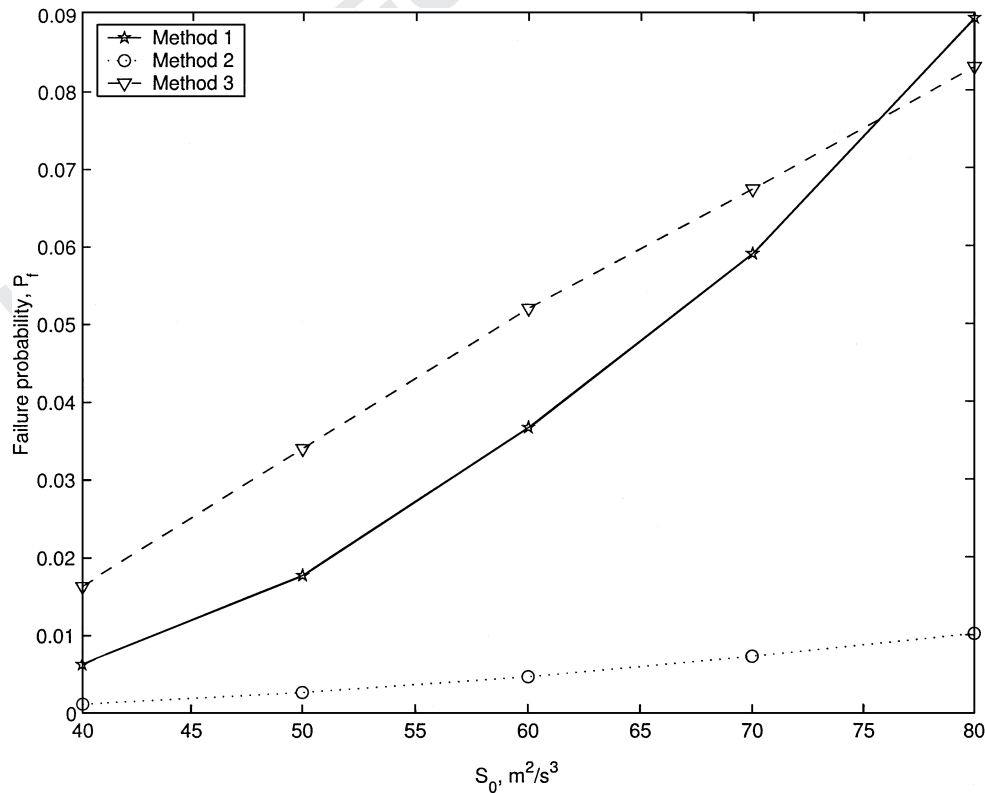


Figure 3. Exceedance probability estimates for linear random structure under non-stationary support excitations; example 2.

10 *S. Gupta and C. S. Manohar*

fitted response surface is taken to be 3000. The number of $g(\mathbf{X})$ evaluations required in Methods 1–3 are respectively 3000, 51 and 3723.

4.3. EXAMPLE 3: RANDOMLY PARAMETERED BEAM WITH MATERIAL AND GEOMETRIC NONLINEARITY

In this example, the time-variant reliability of a support for a fire-fighting water pipeline in a nuclear power plant, is studied under seismic excitations. The support, built up of two channel sections (see Figure 4), is modeled as a cantilever beam. In this figure, $F(t)$ denotes the reaction force transmitted from the piping structure to the pipe support structure. This force itself is obtained by a detailed FE analysis of the piping structure and the details of this calculation have been presented elsewhere [32]. Figure 5 shows the PSD of the stationary component of the force $F(t)$. The fire-fighting water pipeline is considered to be the primary structure under earthquake excitations and the support is assumed to be the secondary structure. Consequently, the pipe is assumed to impart a random force $F(t)$ at the tip of the beam, which is characterized by its PSD $S_{FF}(\omega)$; see Figure 5.

The reliability of the support against ultimate collapse is studied. For the support to fail, a plastic hinge needs to form at the root of the cantilever beam. Thus, the state of the stress at the root needs to be examined. For a combined state of stress in metals, the octahedral shearing stress τ_{oct} , also termed the effective stress and Von Mises stress, is the metric which is generally used for characterizing yielding as well as material hardening [33, 34]. In this problem, the yield surface is assumed to follow the Von Mises yield theory. The material behaves linearly for $\tau_{oct} < \sigma_y$, where σ_y denotes the Von Mises yield stress. When $\tau_{oct} > \sigma_y$, material yielding occurs and it starts behaving elasto-plastically, characterized by a nonlinear stress-strain relationship. A mixed work hardening rule are assumed such that effects of both isotropic and kinematic hardening are considered. Thus, the yield surface undergoes translation as well as expansion, which causes changes in the limits of linear material behavior, characterized by σ_y . In this study, however, strain-rate effects on work hardening have not been considered. When τ_{oct} reaches the ultimate capacity of the material, σ_u , the material fails, leading to the formation of a plastic hinge.

Assumptions based on small deformation theory are relaxed and effects of large deformations are considered in this problem. This introduces geometric nonlinearities in the structure stiffness matrix. The structural analyses is carried out using professionally available finite element software (NISA). The structure is discretized into a 744-noded structure using 360 solid elements, each node having 3 degrees of freedom. Time integration, following Newmark's scheme, has been used to obtain the time history of τ_{oct} at the root of the cantilever beam. The field equations are nonlinear differential

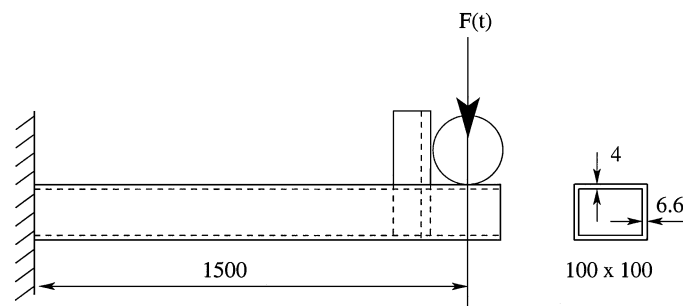


Figure 4. Schematic diagram of the support for the fire-water system in a nuclear power plant; example 3. All dimensions are in mm.

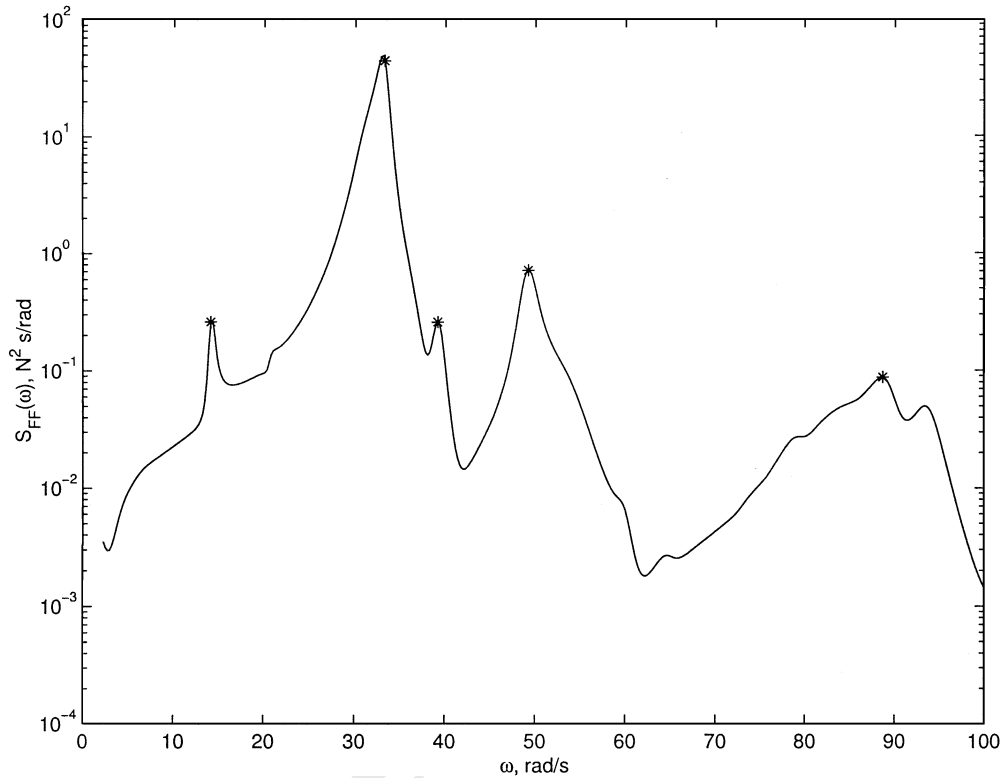


Figure 5. Power spectrum density function for force in example 3; * represents ω_k in Equation (2).

276 equations which require an incremental solution strategy based on iterative methods. In this example,
 277 the full Newton–Raphson method has been used. For a particular time instant, t , the equilibrium state
 278 of the system is thus obtained by an iterative procedure. At the end of each iteration, the solution is
 279 checked for convergence in terms of norms of displacement, the out-of-balance (residual) force vector
 280 and the increment in internal energy during each iteration, before progressing to the next time instant.
 281 Convergence tolerances on the displacement norm, residual force and the internal energy norm have all
 282 been taken to be equal to 0.001.

283 The loading is assumed to have a static and a dynamic component. The static component takes into
 284 account the effect of dead load of the pipe and is equal to 250 N. The dynamic component, arising
 285 due to earthquake excitations, is assumed to be a zero-mean, non-stationary, Gaussian random process.
 286 Using Equations (2) and (3), non-stationary time histories for the forcing function have been generated
 287 from the PSD in Figure 5. The effect of the PSD beyond 100 rad/s has been assumed to be negligible.
 288 The choice of ω_k have been dictated by the peaks observed in Figure 5, denoted by (*), and have been
 289 taken to be 14.12, 33.30, 39.21, 49.26 and 88.72 rad/s, respectively. The parameters A_i ($i = 1, 2, 3$)
 290 in Equation (3) have been taken to be 10.8448, 0.35 and 0.80, respectively. The period of interest has
 291 been taken equal to the time duration of the excitation T , which is 20 s. The yield stress σ_y and the
 292 ultimate stress σ_u are considered to be lognormal random variables with the mean, respectively, being
 293 250 N/mm² and 300 N/mm² and coefficients of variation taken to be 0.03. The performance function
 294 is defined as in Equation (5) where $V(t) = \tau_{oct}$ and $\alpha = \sigma_u$. Here, \mathbf{X} denotes the 12-dimensional vector
 295 of random variables. The structural material is assumed to have mass density 7850 kg/m³, Young’s
 296 modulus (E) 2.018×10^5 N/m² and the work hardening parameter is 1.0866×10^5 . \mathbf{C} is taken to be

Table 2. Exceedance probability estimates for example 3.

Method	$S_0 = 117.07 \text{ N}^2 \cdot \text{s/rad}$	$S_0 = 351.21 \text{ N}^2 \cdot \text{s/rad}$
1	0.1100	0.6900
2	0.0515	0.2998
3	0.1324	0.6492

proportional to linear mass and stiffness matrices (without considering geometric nonlinearities), with the mass and stiffness proportional constants being 0.19 and 0.0021, respectively.

The numbers of $g(\mathbf{X})$ evaluations required in Methods 2 and 3 are respectively, 51 and 1887. To keep the computational time within reasonable limits, only 100 samples were used while implementing Method 1. The algorithm parameters considered in Method 3 are $k = 3$, $l = 2$ and $h = 3$. The number of samples for Monte Carlo simulations on the fitted response surface is taken to be 2×10^4 . Estimates of the failure probabilities computed by Methods 1–3 are provided in Table 2 for $S_0 = 117.07$ and $351.21 \text{ N}^2 \text{ s/rad}$, where S_0 is the variance of $F(t)$.

4.4. DISCUSSION OF NUMERICAL EXAMPLES

In all three examples, the failure probability estimates obtained from Method 3 are found to be in fairly good agreement with those from Method 1. This is in contrast to the estimates obtained from Method 2, which have been shown [28, 31] to be highly sensitive to the algorithm parameters, particularly for nonlinear problems. Moreover, the accuracy of the improved response surface Method is found to be better than Method 2, particularly when there are multiple design points and/or regions which have significant contributions to the failure probability, the existence of which cannot be known beforehand.

The better accuracy achieved in Method 3, in comparison to Method 2, comes at the cost of more of $g(\mathbf{X})$ evaluations, as can be observed from the three numerical examples. The number of $g(\mathbf{X})$ evaluations required in Method 3 is dictated by the geometry of the limit surface and is independent of P_f to be estimated. This is, however, in contrast to Method 1, where the required number of $g(\mathbf{X})$ evaluations varies approximately as $10/P_f$, and hence increases for lower failure probabilities. It should be noted that the CPU time required in performing Monte Carlo simulations on the fitted response surface in Method 3 is negligible in comparison to the computational effort expended in fitting the response surface, especially when the performance function evaluations require significant computer time. Thus, for low failure probabilities, the improved response surface method can be economical in comparison with full scale Monte Carlo simulations.

5. Concluding Remarks

Estimates of reliability of structures under random dynamic loads are obtained from the probability of exceedance of response processes over a specified time duration across predefined thresholds. The computation of these exceedance probabilities requires an explicit knowledge of the mean outcrossing rate of the response process which, in turn, requires a knowledge of joint distribution of the response and its derivative. In most structural reliability problems, the response processes are non-Gaussian and their joint PDF and mean outcrossing rates are difficult to determine. In this study, an improved response surface method has been shown to provide an alternative computational procedure for obtaining exceedance probabilities. The problem has been formulated in the random variable space, which

331 bypasses the need to determine the probability distributions of the structure response processes. The
 332 method can easily be integrated with professionally available finite element softwares, which allows
 333 detailed modeling of the structure and loads. Thus, complexities arising out of geometric and material
 334 nonlinear behavior, randomness in the structural properties, and the non-stationary nature of excitation
 335 can be handled. The computational effort required in the improved response surface method can be
 336 economical in comparison to Monte Carlo simulations, when estimates of low failure probabilities are
 337 desired and when the evaluation of the performance function requires significant computer time.

338 Acknowledgements

339 The work reported in this paper forms part of a research project entitled 'Seismic probabilistic safety
 340 assessment of nuclear power plant structures', funded by the Board of Research in Nuclear Sciences,
 341 Department of Atomic Energy, Government of India.

342 References

- 343 1. Galambos, J., *The Asymptotic Theory of Extreme Order Statistics*, Wiley, New York, 1978.
- 344 2. Castillo, E., *Extreme Value Theory in Engineering*, Academic Press, Boston, 1988.
- 345 3. Kotz, S. and Nadarajah, S., *Extreme Value Distributions*, Imperial College Press, London, 2000.
- 346 4. Nigam, N. C., *Introduction to Random Vibrations*, MIT Press, Massachusetts, 1983.
- 347 5. Roberts, J. B., 'First passage probabilities for randomly excited systems: Diffusion methods', *Probabilistic Engineering*
 348 *Mechanics* **1**, 1986, 66–81.
- 349 6. Madsen, H., 'Extreme value statistics for nonlinear load combination', *Journal of Engineering Mechanics, ASCE*, 1985,
 350 1121–1129.
- 351 7. Segalman D., Fulcher, C., Reese, G., and Field, R., 'An efficient method for calculating r.m.s. Von Mises stress in a random
 352 vibration environment', *Journal of Sound and Vibration* **230**, 2000, 393–410.
- 353 8. Segalman, D., Reese, R., Field, C., and Fulcher, C., 'Estimating the probability distribution of Von Mises stress for structures
 354 undergoing random excitation', *Journal of Vibrations and Acoustics ASME* **122**, 2000, 42–48.
- 355 9. Reese, G., Field, R., and Segalman, D., 'A tutorial on design analysis using Von Mises stress in random vibration
 356 environments', *The Shock and Vibration Digest* **32**(6), 2000, 466–474.
- 357 10. Breitung, K. and Rackwitz, R., 'Nonlinear combination of load processes', *Journal of Structural Mechanics* **10**,
 358 1982, 145–166.
- 359 11. Pearce, H. T. and Wen, Y. K., 'On linearization points for nonlinear combination of stochastic load processes', *Structural*
 360 *Safety* **2**, 1985, 169–176.
- 361 12. Wen, Y. K., *Structural Load Modeling and Combination for Performance and Safety Evaluation*, Elsevier, Amsterdam, 1990.
- 362 13. Khuri, A. I. and Cornell, J. A., *Response Surfaces: Design and Analyses*, Marcel and Dekker, New York, 1997.
- 363 14. Myers, R. H. and Montgomery, D. C., *Response Surface Methodology: Process and Product Optimization Using Designed*
 364 *Experiments*, Wiley, New York, 1995.
- 365 15. Wong, F. S., 'Uncertainties in dynamic soil-structure interaction', *Journal of Engineering Mechanics, ASCE* **110**, 1984,
 366 308–324.
- 367 16. Wong, F. S., 'Slope stability and response surface method', *Journal of Geotechnical Engineering, ASCE* **111**, 1985, 32–53.
- 368 17. Faravelli, L., 'Response surface approach for reliability analysis', *Journal of Engineering Mechanics, ASCE* **115**(12), 1989,
 369 2763–2781.
- 370 18. Faravelli, L., 'Structural reliability via response surface' in *Proceedings of IUTAM Symposium on Nonlinear Stochastic*
 371 *Mechanics*, N. Bellomo and F. Casciati (eds.), Springer, Verlag, 1992, pp. 213–223.
- 372 19. Yao, T. H.-J. and Wen, Y. K., 'Response surface method for time-variant reliability analysis', *Journal of Engineering*
 373 *Mechanics ASCE* **122**, 1996, 193–201.
- 374 20. Bucher, C. G. and Bourgund, U., 'A fast and efficient response surface approach for structural reliability problem', *Structural*
 375 *Safety* **7**, 1990, 57–66.
- 376 21. Rajashekhar, M. R. and Ellingwood, B. R., 'A new look at the response surface approach for reliability analysis', *Structural*
 377 *Safety* **12**, 1993, 205–220.
- 378 22. Rajashekhar, M. R. and Ellingwood, B. R., 'Reliability of reinforced concrete cylindrical shells', *Journal of Structural*
Engineering, ASCE **121**(5), 1995, 336–347.

14 *S. Gupta and C. S. Manohar*

23. Liu, Y. W. and Moses, F., 'A sequential response surface method and its application in the reliability analysis of aircraft structural systems', *Structural Safety* **16**, 1994, 39–46. 379
380
24. Kim, S.-H. and Na, S.-W., 'Response surface method using vector projected sampling points', *Structural Safety* **19**(1), 1997, 3–19. 381
382
25. Brenner, C. E. and Bucher, C. G., 'A contribution to the SFE-based reliability assessment of nonlinear structures under dynamic loading', *Probabilistic Engineering Mechanics* **10**, 1995, 265–273. 383
384
26. Zhao, Y. G., Ono, T., and Idota, H., 'Response uncertainty and time-variant reliability analysis for hysteretic mdf structures', *Earthquake Engineering and Structural Dynamics* **28**, 1999, 1187–1213. 385
386
27. Guan, X. L. and Melchers, R. E., 'Multitangent-plane surface method for reliability calculation', *Journal of Engineering Mechanics, ASCE* **123**(10), 1997, 996–1002. 387
388
28. Guan, X. L. and Melchers, R. E., 'Effect of response surface parameter variation on structural reliability estimation', *Structural Safety* **23**(4), 2001, 429–444. 389
390
29. Breitung, K. and Faravelli, L., 'Response surface methods and asymptotic approximations', in *Mathematical Models for Structural Reliability Analysis*, F. Casciati, and J. B. Roberts (eds.), Ch. 5, CRC Press, Boca Raton, FL, 1996. 391
392
30. Gupta, S. and Manohar, C. S., 'Development of multivariate extreme value distributions for random vibration applications', *Journal of Applied Mechanics, ASME*, 2003, under review. 393
394
31. Gupta, S. and Manohar, C. S., 'An improved response surface method for the determination of failure probability and importance measures', *Structural Safety*, 2003, in press. 395
396
32. Manohar, C. S. and Gupta, S., 'Seismic probabilistic safety assessment of nuclear power plant structures', Project report, funded by Board of Research in Nuclear Sciences, 2003. 397
398
33. Chen, W. F. and Han, D. J., *Plasticity for Structural Engineers*, Springer-Verlag, New York, 1988. 399
34. Chakrabarty, J., *Theory of Plasticity*, McGraw-Hill, Singapore, 1998. 400

Q2

Q2

UNCORRECTED PROOF

Queries

Q1. Au: Please provide Vol No.

Q2. Au: Pls. update.

UNCORRECTED PROOF